Transition Met Chem (2010) 35:787–794
DOI 10.1007/s11243-010-9394-6

Supramolecular cobalt(II) complexes: syntheses, crystal structures and solvent effects

**Wen-Kui Dong · Li Li · Yin-Xia Sun ·
Jun-Feng Tong · Jian-Chao Wu**

Received: 12 April 2010 / Accepted: 25 June 2010 / Published online: 11 July 2010

Abstract Two Co^{II} complexes, namely $\{[CoL(MeOH)(\mu\text{-}OAc)]_2Co\}\cdot 2MeCN\cdot 2MeOH$ (**1**) and $\{[CoL(EtOH)(\mu\text{-}OAc)]_2Co\}\cdot 3EtOH$ (**2**) (H_2L=3,3′-dimethoxy-2,2′-[(1,3-propylene) dioxybis(nitrilomethylidyne)]diphenol), have been synthesized and characterized by X-ray crystallography. Both complexes contain octahedral coordination geometries, comprising three Co^{II} atoms, two deprotonated bisoxime L^{2-} units in which four μ-phenoxo oxygen atoms form two [CoL(X)] (X = MeOH or EtOH) units, two acetate ligands coordinated to three Co^{II} centers through Co–O–C–O–Co bridges, and coordinated and non-coordinated solvent. Both complexes exhibit 2D supramolecular networks through different intermolecular hydrogen-bonding interactions.

Introduction

The self-assembly and synthesis of metal–organic complexes with supramolecular architectures is now a mature research field [1]. The development of new metal–organic complexes can provide new topologies for functional materials, in which pore size, coordination forms and functionality are all important variables [2]. Supramolecular complexes in which the metal centers are bridged through organic ligands are of much current interest, because of their enormous variety of structural topologies and as well as their potential applications in optoelectronics, magnetism and catalysis [3–10]. This subject is currently being pursued in our research, including the use of functional oxime groups and study of the magnetic, photoelectric and catalytic properties of such complexes.

To generate target complexes by design, a judicious choice of ligands is required in order to control the supramolecular interactions. In general, ligands with features such as rigidity and symmetry are suitable for obtaining coordination supramolecules. With this in mind, we have explored Salen-type bisoxime ligands. These can provide N and O donor sites, which together with aromatic rings may form hydrogen bonds and π–π stacking interactions to extend and stabilize the resulting framework. Hence, diverse supramolecular structures may result from this interesting ligand.

Herein, two trinuclear Co^{II} complexes, namely $\{[CoL(MeOH)(\mu\text{-}OAc)]_2Co\}\cdot 2MeCN\cdot 2MeOH$ (**1**) and $\{[CoL(EtOH)(\mu\text{-}OAc)]_2\text{-}Co\}\cdot 3EtOH$ (**2**) (H_2L = 3,3′-dimethoxy-2,2′-[(1,3-propylene)dioxybis(nitrilomethylidyne)]diphenol), have been synthesized and characterized. X-ray crystallographic analyses reveal that the structures of the complexes are pseudo-isostructural, in that they are both trinuclear, with two acetates coordinated to three Co^{II} atoms through Co–O–C–O–Co bridges and four μ-phenoxo oxygen atoms from two [CoL(X)] (X = MeOH or EtOH) units also coordinated to Co^{II}.

Experimental

4-Methoxy-2-hydroxybenzaldehyde (≥98%) from Alfa Aesar was used without further purification. The other reagents and solvents were analytical grade reagents from Tianjin Chemical Reagent Factory and were used without further purification. Elemental analyses for Co were determined with an IRIS ER/S·WP-1 ICP atomic emission spectrometer. C, H and N analyses were obtained with a

W.-K. Dong (✉) · L. Li · Y.-X. Sun · J.-F. Tong · J.-C. Wu
School of Chemical and Biological Engineering, Lanzhou
Jiaotong University, 730070 Lanzhou, Gansu, China
e-mail: dongwk@126.com

GmbH VariuoEL V3.00 automatic elemental analyzer. FTIR spectra were recorded on a VERTEX70 FTIR spectrophotometer, with samples prepared as KBr (500–4,000 cm^{-1}) or CsI (100–500 cm^{-1}) pellets. UV–vis spectra were taken on a Shimadzu UV-240 spectrophotometer. 1H NMR spectra were recorded on a Mercury-400BB spectrometer at room temperature using $CDCl_3$ as solvent. Electrolytic conductance measurements were made with a DDS-11A type conductivity bridge using 1.0×10^{-3} mol L^{-1} solutions in DMF at room temperature. Melting points were measured with a microscopic melting point apparatus made by the Beijing Taike Instrument Limited Company, and the thermometer was uncorrected. TG-DTA analyses were carried out at a heating rate of 5 °C/min in the temperature range 25–900 °C on a ZRY-1P thermoanalyzer, using an Al_2O_3 crucible.

Synthesis of H_2L

1,3-Bis(aminooxy)propane was synthesized by a similar method to that reported earlier [11–13]. 3,3′-Dimethoxy-2,2′-[(1,3-propylene)dioxybis(nitrilomethylidyne)]diphenol (H_2L) was synthesized according to a method analogous to that reported earlier [12–14]. To an ethanol solution (10 mL) of 4-methoxy-2-hydroxybenzaldehyde (62.5 mg, 0.41 mmol) was added an ethanol solution (5 mL) of 1,3-bis(aminooxy)propane (21.8 mg, 0.21 mol). The mixture was stirred at 55 °C for 4 h. After cooling to room temperature, the precipitate was filtered off and washed successively with ethanol and ethanol/*n*-hexane (1:3, V/V). The product was dried under vacuum, and obtained as a colorless crystalline solid (Yield 481 mg, 63%, M.P. 97–98 °C). ^1H NMR (400 MHz, $CDCl_3$) 2.12 (t, $J = 6.6$ Hz, 2H), 3.81 (s, 6H), 4.26 (t, $J = 6.20$ Hz, 4H), 6.46 (d, $J = 2.4$ Hz 2H), 6.50 (d, $J = 2.4$ Hz 2H), 6.98 (s, 2H), 8.09 (s, 2H), 10.00 (s, 2H). Found: C, 61.0; H, 6.0; N, 7.3. Calcd. for $C_{19}H_{22}N_2O_6$ (%): C, 61.0; H, 5.9; N, 7.5.

Preparation of complex **1**

A solution of $Co(OAc)_2 \cdot 4H_2O$ (8.0 mg, 0.032 mmol) in methanol (4 mL) was added dropwise to a solution of H_2L (12.1 mg, 0.032 mmol) in acetonitrile (4 mL). The color of the solution immediately turned yellow, and the mixture was allowed to stand at room temperature for about 1 week. After the solvent was partially evaporated, it separated out several reddish-brown block-shaped single crystals suitable for X-ray crystallographic analysis. Found: C, 48.1; H, 5.5; N, 6.6; Co, 14.1. Calcd. for $C_{50}H_{68}Co_3N_6O_{20}$ (%): C, 48.1; H, 5.5; N, 6.7; Co, 14.2.

Preparation of complex **2**

The synthesis of complex **2** was similar to complex **1**, except that $Co(OAc)_2 \cdot 4H_2O$ was dissolved in ethanol. Found: C, 49. 4; H, 5.8; N, 4.7; Co, 13.7. Calcd. for $C_{52}H_{76}Co_3N_4O_{21}$ (%): C, 49.2; H, 6.0; N, 4.4; Co, 13.9.

Crystal structure determinations

Single crystals suitable for data collection were selected and glued to the tip of a glass fiber. The determination of the crystal structures at 153 K and 298 K for complexes **1** and **2** were carried out with a Rapid Auto Version 3.0 Rigaku RAXIS-RAPID detector and Bruker Smart APEX II CCD diffractometer, respectively. Both diffractometers used graphite-monochromated Mo–Kα radiation ($\lambda = 0.71073$ Å). The LP factor semi-empirical absorption corrections were applied using the SADABS program [15]. The structures were solved by direct methods and refined by the full-matrix least-squares method on F^2 using the SHELXTL crystallographic software package [16]. All non-hydrogen atoms were refined with anisotropic thermal parameters. Hydrogen atoms were placed in calculated positions and included in the final cycles of refinement using a riding model. A summary of the key crystallographic information is given in Table 1, and the final positional and thermal parameters are available as supplementary material.

Results and discussion

Two solvent-induced supramolecular Co^{II} complexes have been synthesized and characterized (Scheme 1). Both complexes are soluble in DMF, DMSO and $CHCl_3$, but not soluble in EtOH, MeOH, MeCN, acetone, THF, ethyl acetate or n-hexane. Noticeably, they are both unstable in air at room temperature. The free ligand is soluble in all of the aforementioned solvents. The molar conductance values of complexes **1** and **2** in 1.0×10^{-3} mol dm^{-3} DMF solutions are 15.5 and 15.2 S cm^2 mol^{-1}, respectively, indicating that both are non-electrolytes. This implies that all of the acetate groups in both complexes are held in the coordination sphere in solution or solid state.

Principal FTIR bands for H_2L and its complexes **1** and **2** are given in Table 2. The free ligand H_2L exhibits Ar–O and C=N stretching bands at 1,223 and 1,613 cm^{-1}, which are shifted to lower frequencies by *ca.* 2 and 7 cm^{-1} for complex **1** (4 and 2 cm^{-1} for complex **2**) upon complexation. This lowering of energy results from the Co–O and Co–N interactions upon complexation and is similar to that reported for other Co^{II} complexes [17]. In addition, the

Table 1 Crystal data and structure refinement parameters for complexes **1** and **2**

Complex	**1**	**2**
Empirical formula	$C_{50}H_{68}Co_3N_6O_{20}$	$C_{52}H_{76}Co_3N_4O_{21}$
Formula weight (g mol^{-1})	1249.89	1269.96
Crystal system	Monoclinic	Triclinic
Space group	C2/c	$P\bar{1}$
Temperature (K)	153(2) K	298(2) K
Unit cell dimensions(Å, °)	$a = 25.1482(7)$	$a = 11.476(1)$
	$b = 12.3318(5)$	$b = 11.901(1)$
	$c = 19.8322(6)$	$c = 11.965(1)$
	$\alpha = 90$	$\alpha = 70.911(1)$
	$\beta = 115.801(1)$	$\beta = 72.603(1)$
	$\gamma = 90$	$\gamma = 86.811(2)$
V (Å^3)	5537.3(3)	1472.0(2)
Z	4	1
Calculated density (mg/m^3)	1.499	1.433
Absorption coefficient (mm^{-1})	0.969	0.913
θ range for data collection (°)	3.14–27.48	1.81–25.02
Limiting indices	$-32 \le h \le 30$, $-15 \le k \le 16$, $-24 \le l \le 25$	$-13 \le h \le 13$, $-11 \le \mathrm{k} \le 14$, $-9 \le l \le 14$
$F(000)$	2,604	665
Crystal size (mm)	0.58 × 0.57 × 0.37	0.38 × 0.28 × 0.27
Reflection collected/unique	41,875/6,326 [R(int) = 0.0376]	7,706/5,120 [R(int) = 0.0177]
Refinement method	Full-matrix least squares on F^2	Full-matrix least squares on F^2
Data/restraints/parameters	6,326/0/373	5,120/0/429
Goodness of fit on F^2	1.020	1.005
Final R indices [$I > 2\sigma$(I)]	$R_1 = 0.0332$, $wR_2 = 0.0862$[a]	$R_1 = 0.0370$, $wR_2 = 0.0908$[b]
R indices (all data)	$R_1 = 0.0368$, $wR_2 = 0.0897$	$R_1 = 0.0572$, $wR_2 = 0.1053$
Max, min $\Delta\rho$ (eÅ^{-3})	0.7157 and 0.6033	0.7907 and 0.7230
CCDC	652641	751664

[a] $w = 1/[\sigma^2(F_o^2) + (0.0483P)^2 + 9.1774P]$, [b] $w = 1/[\sigma^2(F_o^2) + (0.0472P)^2 + 0.7277P]$, where $P = (F_o^2 + 2F_c^2)/3$

Scheme 1 Synthesis of the complexes, R = Me (**1**) or Et (**2**)

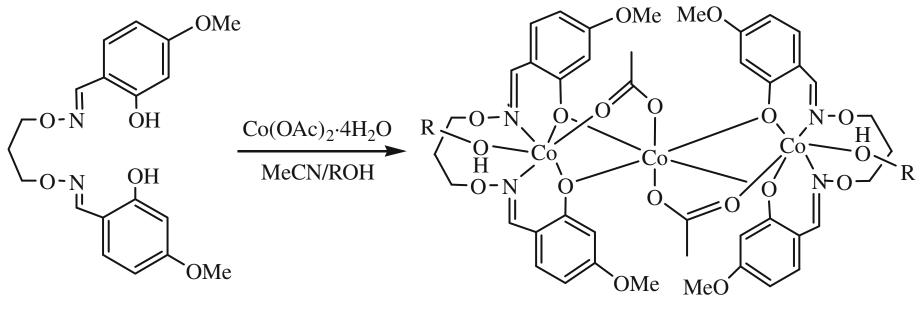

Table 2 Principal FTIR bands for H_2L and complexes **1** and **2** (cm^{-1})

Compound	$\nu_{(Ar–O)}$	$\nu_{(C=N)}$	$\nu_{(Co–N)}$	$\nu_{(Co–O)}$	$\nu_{(C=C)}$ benzene ring skeleton
H_2L	1,223	1,613	–	–	1,570, 1,514, 1,460
Complex **1**	1,221	1,606	473	411	1,539, 1,491, 1,418
Complex **2**	1,219	1,611	474	413	1,585, 1,535, 1,450

infrared spectra of complexes **1** and **2** show the expected absorption band due to the stretching modes of methanol or ethanol at *ca.* 3,432 and 3,425 cm^{-1}, respectively.

The far-infrared spectra of complexes **1** and **2** were also obtained in the region of 500–100 cm^{-1}. The IR spectrum of complex **1** shows ν(Co–O) and ν(Co–N) vibrations at 411 and 473 cm^{-1}, respectively (413 and 474 cm^{-1} for complex **2**), which are consistent with the literature values

[18–20]. Analogous bands are not observed in the spectrum of the free ligand. As pointed out by Percy and Thornton [21], the precise metal–oxygen and metal–nitrogen assignments are often difficult.

The UV–Vis absorption spectrum of H_2L in DMF solution exhibits two intense peaks at around 278 and 311 nm. These are the characteristic peaks for any Salen-type ligands due to π–π* transitions [22, 24]. However, there is no absorption around 400 nm, which is usually seen for Salen derivatives in the keto-NH form [23, 25].

The absorption peak of H_2L at 278 nm is shifted to lower energy by *ca.* 13 and 5 nm in complexes **1** and **2**, respectively, consistent with coordination of the Co^{II} atoms to L^{2-} ligands. The peak of H_2L at 311 nm is absent for complexes **1** and **2**. However, new absorptions are observed at 339 and 346 nm, respectively, and assigned to be the $n - \pi^*$ charge transfer transition from the filled pπ orbital of the bridging phenolic oxygen to the vacant d-orbital of the Co^{II} atoms [24].

The thermal decomposition of complex **1** can be divided into four stages. The first stage is at 45–67 °C. The TG curve shows that the weight loss corresponding to this temperature range is 11.1%, which roughly coincides with the value of 11.7%, calculated for the loss of non-coordinated solvent (two of methanol and two of acetonitrile) from complex **1**. The second stage starts from 84 to 97 °C with a weight loss of 4.8%, which corresponds to the loss of two methanol ligands (theoretical mass loss 5.1%). The third stage degradation is in the range of 216–252 °C with a mass loss of 10.2%, assigned to loss of two coordinated acetate groups with theoretical value of 9.4%. The residue remains stable up to 334 °C, when the fourth weight loss starts. The TG curve shows around 79% total mass loss at 800 °C, indicating complete removal of the organic part of the compound. The residue was CoO with a value of 21% (theoretical value 18.0%).

Thermal decomposition of complex **2** also occurs in four stages. The initial weight loss occurs in the range 45–53 °C. The TG curve shows that weight loss corresponding to this temperature range is 10.3%, consistent with 10.9% calculated for loss of three non-coordinated ethanol molecules. The second stage is 88–102 °C with weight loss of 7.0%, assigned to the loss of two ethanol ligands (theoretical mass loss, 7.3%). The third stage of degradation is in the range 216–252 °C with mass loss of 9.8%, in which two coordinated acetate anions are lost with theoretical value of 9.3%. The solid remains stable up to 348 °C, whereupon fourth weight loss commences. Subsequently, continuous mass loss was observed up to 800 °C. At this temperature, CoO is formed. The total mass loss found (82.3%) was consistent with the calculated value (82.3%).

Description of the crystal structures

In order to determine the correct configuration of the complexes, X-ray crystallographic studies have been realized for complexes **1** and **2**. Complex **1** crystallizes in the monoclinic space group C2/c, and consists of two L^{2-} ligands, three Co^{II} atoms, two acetate anions, two coordinated methanol molecules, two non-coordinated methanol and two non-coordinated acetonitrile molecules. Selected bond lengths and angles are listed in Table 3.

As shown in Fig. 1, the two terminal Co^{II} atoms (Co1 and $Co1^{\#1}$) are both located in the cis-N_2O_2 coordination cavity of the L^{2-} ligands, and carboxylate oxygen atom O7 from the μ-acetato bridge and oxygen atom O9 from the methanol ligand are also coordinated to Co1 in the axial positions. Furthermore, the dihedral angle between the coordination planes of O1–Co1–N1 and O2–Co1–N2 is 4.50(2)°, indicating slight distortion toward octahedral geometry from the square planar structure. Because Co1 and $Co1^{\#1}$ are symmetry related, they will have identical geometries [26]. In addition, the coordination sphere of the central Co^{II} atoms (Co2) is completed by quadruple

Table 3 Selected bond distances (Å) and bond angles (°) for complex **1**

Bond lengths			
Co(1)–O(7)	2.051(1)	Co(2)–O(2)	2.076(1)
Co(1)–O(1)	2.055(1)	Co(2)–O(2)$^{\#1}$	2.076(1)
Co(1)–O(2)	2.076(1)	Co(2)–O(1)	2.120(1)
Co(1)–O(9)	2.138(1)	Co(2)–O(1)$^{\#1}$	2.120(1)
Co(1)–N(2)	2.138(2)	Co(2)–O(8)	2.146(1)
Co(1)–N(1)	2.142(2)	Co(2)–O(8)$^{\#1}$	2.146(1)
Bond angles			
O(7)–Co(1)–O(1)	93.46(5)	O(2)–Co(2)–O(2)$^{\#1}$	180.00(6)
O(7)–Co(1)–O(2)	92.01(5)	O(2)–Co(2)–O(1)	77.18(5)
O(1)–Co(1)–O(2)	78.63(5)	O(2)$^{\#1}$–Co(2)–O(1)	102.82(5)
O(7)–Co(1)–O(9)	173.07(5)	O(2)–Co(2)–O(1)$^{\#1}$	102.82(5)
O(1)–Co(1)–O(9)	93.38(5)	O(2)$^{\#1}$–Co(2)–O(1)$^{\#1}$	77.18(5)
O(2)–Co(1)–O(9)	88.29(5)	O(1)–Co(2)–O(1)$^{\#1}$	180.00(1)
O(7)–Co(1)–N(2)	87.60(6)	O(2)–Co(2)–O(8)	90.05(5)
O(1)–Co(1)–N(2)	164.77(5)	O(2)$^{\#1}$–Co(2)–O(8)	89.95(5)
O(2)–Co(1)–N(2)	86.15(5)	O(1)–Co(2)–O(8)	87.48(4)
O(9)–Co(1)–N(2)	85.51(6)	O(1)$^{\#1}$–Co(2)–O(8)	92.52(4)
O(7)–Co(1)–N(1)	93.29(6)	O(2)–Co(2)–O(8)$^{\#1}$	89.95(5)
O(1)–Co(1)–N(1)	84.85(5)	O(2)$^{\#1}$–Co(2)–O(8)$^{\#1}$	90.05(5)
O(2)–Co(1)–N(1)	162.92(5)	O(1)–Co(2)–O(8)$^{\#1}$	92.52(4)
O(9)–Co(1)–N(1)	88.40(5)	O(1)$^{\#1}$–Co(2)–O(8)$^{\#1}$	87.48(4)
N(2)–Co(1)–N(1)	110.28(6)	O(8)–Co(2)–O(8)$^{\#1}$	180.0

Symmetry transformations used to generate equivalent atoms: $^{\#1}-x + 3/2, -y + 3/2, -z + 1$

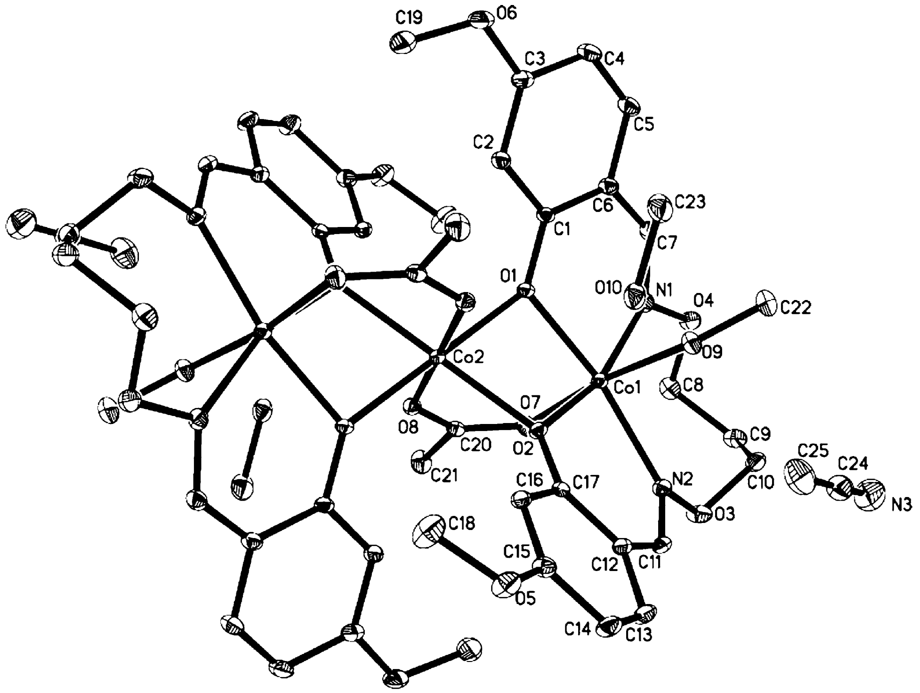

Fig. 1 ORTEP view of the crystal structure of complex **1**. Thermal ellipsoids were drawn at the 30% probability level and hydrogen atoms have been omitted for clarity

μ-phenoxo oxygen atoms from two L^{2-} moieties and double μ-acetato oxygen atoms which adopt a familiar μ–O–C–O fashion. All the six oxygen atoms coordinated to Co2 constitute an octahedral geometry: one acetate anion serves as bridging group for Co1 and Co2 and the other coordinates to $Co1^{\#1}$ and Co2, in both cases via Co–O–C–O–Co bridges. The Co1(or $Co1^{\#1}$) atom in complex **1** is 0.052 Å out of the N_2O_2 coordination plane defined by atoms (N1N2O1O2 or $N1^{\#1}N2^{\#1}O1^{\#1}O2^{\#1}$), while the Co2 atom lies exactly in the corresponding N_2O_2 coordination plane defined by atoms ($O1O2O1^{\#1}O2^{\#1}$). The bond angles around Co1 or $Co1^{\#1}$ in the trans-positions are in the range of 162–173°, while those around Co2 are all 180°, showing that the terminal Co^{II} center has a higher distortion than that of the central one in octahedral geometry.

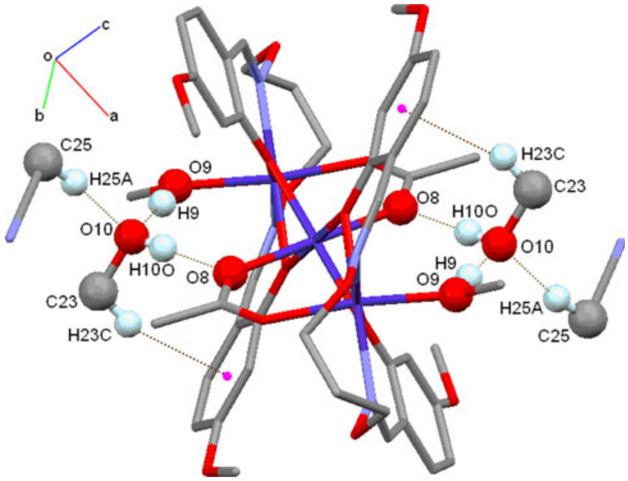

Fig. 2 Hydrogen-bonding interactions of complex **1**

There is an inversion center through the central Co^{II} atom (Co2), and the distance of Co2–O1 (2.1198(1) Å) is longer than that of Co2–O2 (2.076(1) Å) (Table 3), indicating a weaker steric effect. Similar elongations of Co–O bonds have also been observed in the $[Co(Salen)]_2$ dimer [17]. The Co1–N2 (2.1422(2) Å) is slightly longer than Co1–N1 (2.1384(2) Å), which is attributed to the methanol molecule coordinating to the terminal Co^{II} atoms (Co1 and $Co1^{\#1}$) resulting in larger steric hindrance.

In the crystal structure of complex **1**, as shown in Fig. 2, each of two non-coordinated methanol molecules is connected with the two non-coordinated acetonitrile molecules through C25–H25A···O10 hydrogen-bonding interactions (Table 4). Also, the non-coordinated methanol molecules are linked to the inner-sphere units, $\{[CoL(MeOH)(\mu\text{-}OAc)]_2Co\}$, via O10–H10···O8, O9–H9···O10 and C23–H23C···π hydrogen-bonding interactions, and to form a monomer structure of $\{[CoL(MeOH)(\mu\text{-}OAc)]_2Co\}\cdot 2MeCN\cdot 2MeOH$ units. Furthermore, every monomer molecule links four other molecules into an infinite 2D-layer supramolecular structure parallel to the bc crystallographic plane via intermolecular hydrogen bonds between the oxygen atoms of the methoxy group and the methylene groups of O-alkyl chains of L^{2-} ligands in the adjacent molecules (Fig. 3).

The molecular structure of complex **2** is shown in Fig. 4. Selected bond lengths and angles are given in Table 5. Complex **2** crystallizes in the triclinic system, space group $P\bar{1}$ with a linear trinuclear array of three Co^{II} atoms

Table 4 Hydrogen-bonding distances (Å) and bond angles (°) for complexes **1** and **2**

D–H···A	D–H	H···A	D···A	D–H···A
Complex **1**				
O9–H9···O10	0.85	1.77	2.616 (2)	177
O10–H10O···O8^{i}	0.82	1.86	2.680(2)	175
C25–H25A···O10^{ii}	0.98	2.46	3.419(3)	166
C23–H23C···Cg1	0.98	2.89	3.784(2)	153
C8–H8A···O6^{iii}	0.99	2.69	3.473(2)	137
C9–H9A···O5^{iv}	0.99	2.63	3.498(4)	147
Complex **2**				
O9–H9···O10^{v}	0.82	1.825	2.641(3)	173
O10–H10···O8	0.82	1.945	2.761(3)	174
C24–H24B···Cg2^{vi}	0.97	2.71	3.614(5)	156
C2–H2A···O6^{vii}	0.97	2.58	3.339(5)	135
C2–H2B···O2^{viii}	0.97	2.64	3.548(4)	156

Symmetry codes: (i) 3/2 − *x*, 3/2 − *y*, 1 − *z*; (ii) 1 − *x*, *y*, ½ − *z*; (iii) *x*, 2 − *y*, 1/2 + *z*; (iv) *x*, 1 − *y*, 1/2 + *z*; (v) 1 − *x*, 1 − *y*, 1 − *z*; (vi) 1 − *x*, 1 − *y*, 1 − *z*; (vii) 1 + *x*, *y*, *z*; (viii) 2 − *x*, 2 − *y*, −*z*. Cg1 and Cg2 are the centroids of atoms C1–C6 and C13–C18, respectively

coupled by both doubly μ-phenoxo oxygen atoms of L^{2-} ligands plus two acetate anions in the syn–syn bridging mode. All the hexa-coordinated Co^{II} atoms of complex **2** have a slightly distorted octahedral coordinated polyhedron.

The structure of complex **2** is pseudo isostructural with that of complex **1**. Consequently their structural features are very similar except that one of the oxygen atoms in apical positions around the terminal Co^{II} centers is not from the methanol but the ethanol ligand in complex **2**. The dihedral angle between the planes of O5–Co1–N2 and O3–Co1–N1 in complex **2** is 7.96(4)°, which is a little bigger than that of O1–Co1–N1 and O2–Co1–N2 (4.50(2)°) in complex **1**. Furthermore, the terminal atom (Co1 and Co1$^{\#1}$) in complex **2** is 0.062 Å out of the N_2O_2 coordination equatorial plane

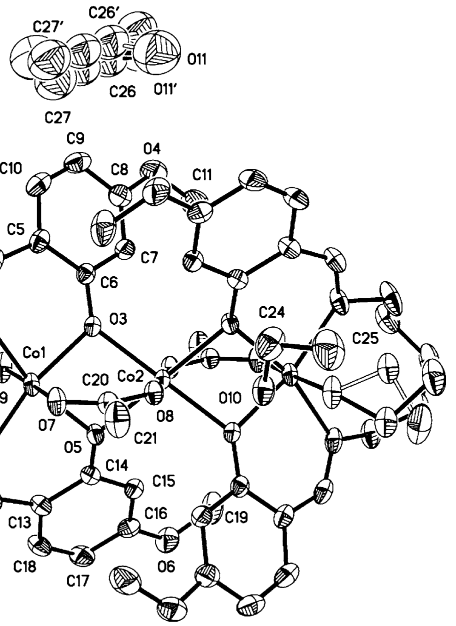

Fig. 4 ORTEP view of the crystal structure of complex **2**. Thermal ellipsoids were drawn at the 30% probability level and hydrogen atoms have been omitted for clarity

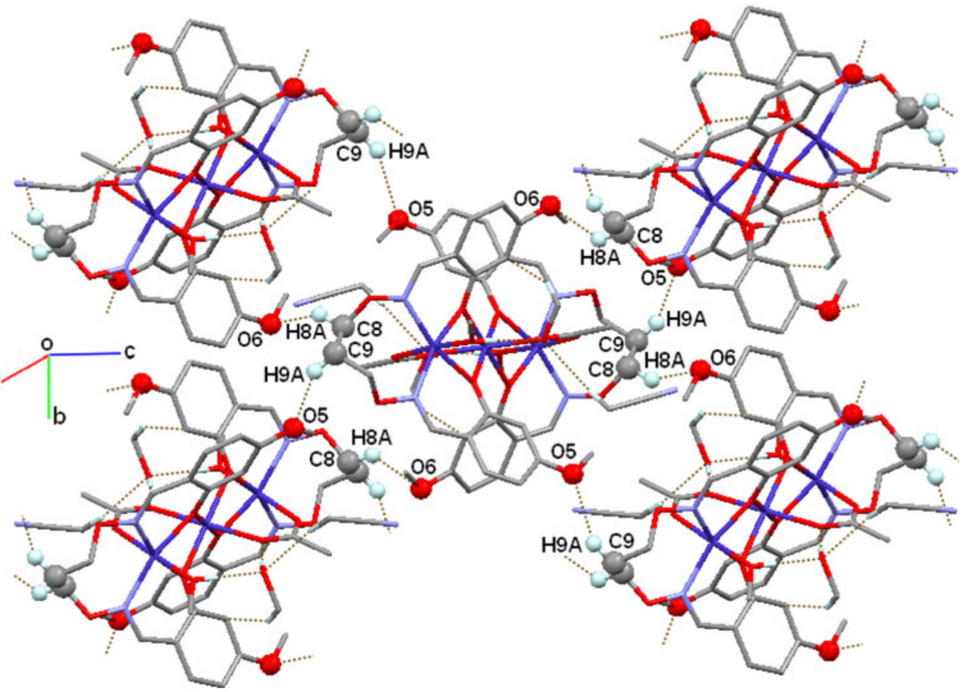

Fig. 3 View of the 2D supramolecular network of complex **1** (hydrogen atoms, except those forming hydrogen bonds, are omitted for clarity)

Table 5 Selected bond distances (Å) and bond angles (°) for complex **2**

Bond lengths			
Co(1)–O(3)	2.039(2)	Co(2)–O(3)	2.097(2)
Co(1)–O(7)	2.054(2)	Co(2)–O(3)$^{\#1}$	2.097(2)
Co(1)–O(5)	2.074(2)	Co(2)–O(5)$^{\#1}$	2.098(2)
Co(1)–N(1)	2.127(3)	Co(2)–O(5)	2.098(2)
Co(1)–N(2)	2.135(3)	Co(2)–O(8)	2.141(2)
Co(1)–O(9)	2.159(2)	Co(2)–O(8)$^{\#1}$	2.141(2)
Bond angles			
O(3)–Co(1)–O(7)	95.59(8)	O(3)–Co(2)–O(3)$^{\#1}$	180.000(1)
O(3)–Co(1)–O(5)	78.98(7)	O(3)–Co(2)–O(5)$^{\#1}$	102.87(7)
O(7)–Co(1)–O(5)	90.71(8)	O(3)$^{\#1}$–Co(2)–O(5)$^{\#1}$	77.13(8)
O(3)–Co(1)–N(1)	86.22(9)	O(3)–Co(2)–O(5)	77.13(8)
O(7)–Co(1)–N(1)	88.7(1)	O(3)$^{\#1}$–Co(2)–O(5)	102.87(7)
O(5)–Co(1)–N(1)	165.05(9)	O(5)$^{\#1}$–Co(2)–O(5)	180.00(7)
O(3)–Co(1)–N(2)	162.21(9)	O(3)–Co(2)–O(8)	88.43(8)
O(7)–Co(1)–N(2)	92.6(1)	O(3)$^{\#1}$–Co(2)–O(8)	91.57(8)
O(5)–Co(1)–N(2)	85.15(9)	O(5)$^{\#1}$–Co(2)–O(8)	91.90(8)
N(1)–Co(1)–N(2)	109.8(1)	O(5)–Co(2)–O(8)	88.10(8)
O(3)–Co(1)–O(9)	86.51(9)	O(3)–Co(2)–O(8)$^{\#1}$	91.57(8)
O(7)–Co(1)–O(9)	176.77(8)	O(3)$^{\#1}$–Co(2)–O(8)$^{\#1}$	88.43(8)
O(5)–Co(1)–O(9)	92.11(9)	O(5)$^{\#1}$–Co(2)–O(8)$^{\#1}$	88.10(8)
N(1)–Co(1)–O(9)	89.0(1)	O(5)–Co(2)–O(8)$^{\#1}$	91.90(7)
N(2)–Co(1)–O(9)	86.1(1)	O(8)–Co(2)–O(8)$^{\#1}$	180.0(1)

Symmetry transformations used to generate equivalent atoms: $^{\#1}-x+1, -y+1, -z+1$

(that of in complex **1** is 0.052 Å), but the central Co2 atom lies in the corresponding O_2O_2 equatorial plane. The bond angles around Co1 or Co1$^{\#1}$ in the trans-positions are in the range of 162–177° in complex **2,** whereas those of complex **1** are in the range of 162–173°, showing that the terminal Co^{II} atom has a higher distortion than the central one in octahedral geometry in both complexes. Furthermore, the distortion around the terminal Co^{II} atoms in complex **2** is stronger than that in complex **1**, perhaps due to larger steric hindrance of the ethanol ligands compared to the methanol ligands.

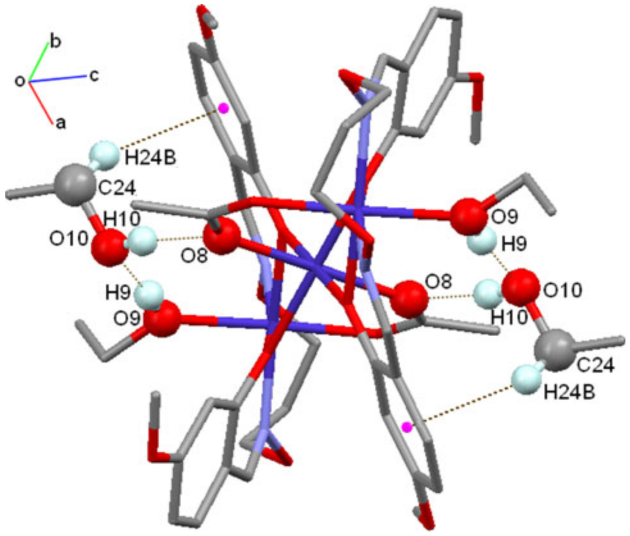

Fig. 5 Hydrogen-bonding interactions of complex **2**

In addition, similar to complex **1**, analysis of the crystal packing of **2** shows a 2D hydrogen-bonding supramolecular network involving intermolecular O10–H10···O8, O9–H9···O10 and C24–H24B···π(Ph, C13–C18) interactions (Fig. 5). Moreover, the monomers are linked by intermolecular C2–H2A···O6 and C2–H2B···O2 hydrogen bond interactions into a 2D supramolecular network structure (Fig. 6).

Solvent effects

For both complexes **1** and **2**, the ratio of L:Co is 2:3. Every terminal Co^{II} atom forms two six-membered rings with two salicylaldoxime moieties and the acetates adopt their familiar role to reinforce the structures by bridging between adjacent Co^{II} atoms. The influence of solvent effect is clearly revealed in selected bond distances and angles for complexes **1** and **2**. In complex **1**, the distance from O9 (coordinated methanol molecule) to the plane of N1–N2–O1–O2 is 2.081(2) Å and O9–Co1 is 2.138(1) Å, so we confirm that Co1 is not coplanar with the N1–N2–O1–O2 plane and slightly deviates toward O7 from the acetate anion. The dihedral angle between N1–Co1–O1 and N2–Co1–O2 is 4.50(2)°. Complex **2** shows that the distance from O9 (ethanol ligand) to the plane of N1–N2–O3–O5 (2.96(2) Å) is shorter than O9–Co1 (2.159(2) Å). As for complex **1**, Co1 is also not coplanar with the N1–N2–O3–O5 plane but slightly deviates toward O7 from the acetate anion. The dihedral angle between N1–Co1–O3 and N2–Co1–O5 is 7.96(4)°. This deviation of Co1 toward O7 in both complexes may be attributed to the electrostatic attraction of acetate. Further, the dihedral angle of the two planes (N1–Co1–O3 and N2–Co1–O5) in complex **2** (7.96(4)°) is bigger than that in complex **1** (4.50(2)°), due to larger steric hindrance of the ethanol ligands than the methanol ligands. Thus, solvent effects in complexes **1** and **2** can explain their slight differences in crystal structures (Scheme 1).

Conclusion

Two trinuclear Co^{II} complexes have been synthesized and characterized. Because of the introduction of different solvent molecules, these complexes present slightly different structural features. Complex **1** has two methanol ligands coordinated to the terminal Co^{II} atoms, while complex **2** has ethanol ligands. The distortion of the

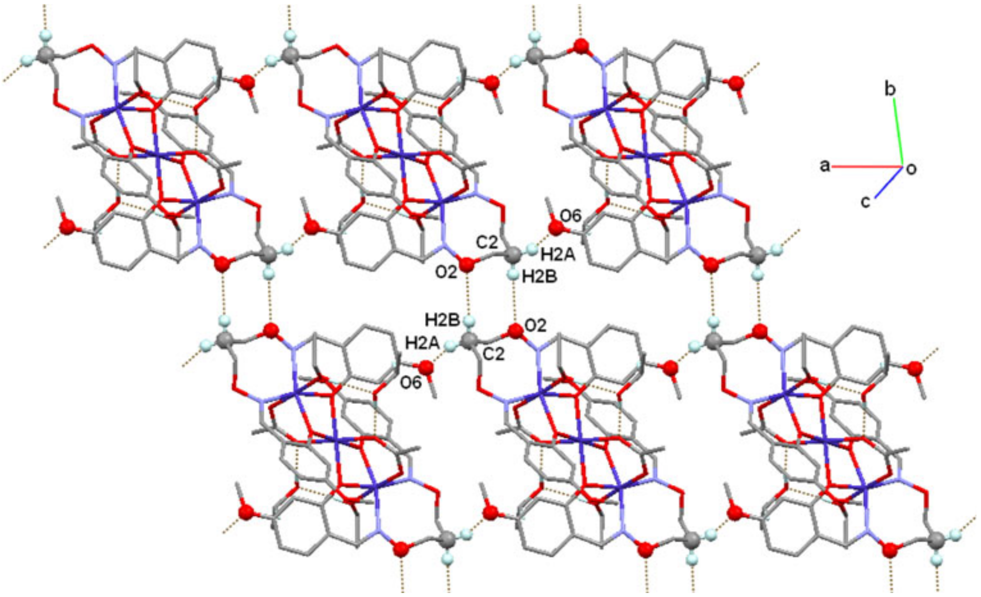

Fig. 6 View of the 2D supramolecular network of complex **2** (hydrogen atoms, except those forming hydrogen bonds, are omitted for clarity)

octahedral coordination geometry around the terminal Co^{II} atoms in complex **2** is stronger than that of complex **1**, suggesting that the steric hindrance of the ethanol ligands is larger than that of the methanol ligands.

Supplementary material

Crystallographic data have been deposited with the Cambridge Crystallographic Data Centre as supplementary publication, No. CCDC 652641 and 751664 for complexes **1** and **2**, respectively. Copies of the data can be obtained free of charge on application to CCDC, 12 Union Road, Cambridge CB2 1EZ, UK (Telephone: +44-01223-762910; Fax: +44-1223-336033; E-mail: deposit @ccdc.cam.ac.uk). These data can be also obtained free of charge at www.ccdc.cam.ac.uk/conts/retrieving.html.

Acknowledgments This work was supported by the Foundation of the Education Department of Gansu Province (No. 0904-11) and the 'JingLan' Talent Engineering Funds of Lanzhou Jiaotong University, which are gratefully acknowledged.

References

1. Braga D, Maini L, Polito M, Tagliavini E, Grepioni F (2003) Coord Chem Rev 246:53–71
2. Saylor SM, Supkowski RM, LaDuca RL (2008) Inorg Chim Acta 361:317–326
3. Han HY, Song YL, Hou HW, Fan YT, Zhu YJ (2006) Chem Soc Dalton Trans 16:1972–1980
4. Braun ME, Steffek CD, Kim J, Rasmussen PG, Yaghi OM (2001) Chem Commun 24:2532–2533
5. Rosi NL, Eddaoudi M, Kim J, O'Keeffe M, Yaghi OM (2002) Cryst Eng Commun 4:401–404
6. Eddaoudi M, Moler DB, Li H, Chen B, Reineke TM, O'Keeffe M, Yaghi OM (2001) Acc Chem Res 34:319–330
7. Chen B, Eddaoudi M, Hyde ST, O'Keeffe M, Yaghi OM (2001) Science 291:1021–1023
8. Kim J, Chen B, Reineke TM, Li H, Eddaoudi M, Moler DB, O'Keeffe M, Yaghi OM (2001) J Am Chem Soc 123:8239–8247
9. Yaghi OM, O'Keeffe M, Ockwig NW, Chae HK, Eddaoudi M, Kim J (2003) Nature 423:705–741
10. Forster PM, Cheetham AK (2004) Microporous Mesoporous Mater 73:57–64
11. Akine S, Dong WK, Nabeshima T (2006) Inorg Chem 45:4677–4684
12. Dong WK, Zhu CE, Wu HL, Yu TZ, Ding YJ (2007) Synth React Inorg Met-Org Nano-Met Chem 37:61–67
13. Dong WK, Feng JH, Yang XQ (2007) Synth React Inorg Met-Org Nano-Met Chem 37:189–192
14. Dong WK, Feng JH (2006) Acta Cryst E62:o3577–o3578
15. Sheldrick GM (1996) SADABS, siemens area detector absorption corrected software. University of Göttingen, Germany
16. Sheldrick GM (1997) SHELXTL NT, version 5.1; program for solution and refinement of crystal structures. University of Göttingen, Germany
17. Delasi R, Holt SL, Post B (1971) Inorg Chem 10:1498–1500
18. Dong WK, Li L, Li CF, Xu L, Duan JG (2008) Spectrochimica Acta Part A 71:650–654
19. Dong WK, Sun YX, Zhang YP, Li L, He XN, Tang XL (2009) Inorg Chim Acta 362:117–124
20. Majumder A, Rosair GM, Mallick A, Chattopadhyay N, Mitra S (2006) Polyhedron 25:1753–1762
21. Percy GC, Thornton J (1973) J Inorg Nucl Chem 35:2319–2327
22. Akine S, Taniguchi T, Nabeshima T (2001) Chem Lett 30:682–683
23. Akine S, Taniguchi T, Dong WK, Nabeshima T (2005) J Org Chem 70:1704–1711
24. Chu ZL, Huang W (2007) J Mol Struct 837:15–22
25. Smith HE (1983) Chem Rev 83:359–377
26. Dong WK, Duan JG, Chai LQ, Liu GL, Wu HL (2008) J Coord Chem 61:1306–1315